Photoassisted amplification of chain-growth in CO_2 hydrogenation: Switching selectivities of heterogeneously catalyzed reactions with light

Henning Becker, Dirk Ziegenbalg*, Robert Güttel*

Institute of Chemical Engineering, Ulm University, Ulm, Germany

Abstract

Selective carbon-carbon bond formation is a major challenge for chemical transformations to meet the global sustainability targets, which requires game-changing concepts instead of further improvement of conventional catalyst materials. In this work, a new paradigm to tune the selectivity of thermal catalytic systems is presented by using light as an external trigger to switch the selectivity from pure reduction to carbon-carbon bond formation. In a ruthenium-catalyzed CO_2 hydrogenation reaction, chain-growth is initiated through irradiation with light, eventually leading to the formation of higher hydrocarbons instead of solely methane. Photoassisted reaction control was differentiated from photokinetic and photothermal effects by sophisticated thermal imaging and kinetic modelling. A light-induced change of the sorption properties of the solid catalyst surface was identified as reason for the changes in selectivity. The results render the exploitation of photoassisted effects as highly potent general strategy for comprehensive reaction control of reactions catalyzed by solids.

Introduction

The selective formation of carbon-carbon bonds is a key requirement for providing the chemical basis for future sustainable materials based on CO_2 utilization.[1] At the same time, high selectivities allow to minimize the energetical burden of separation processes and thereby represent a large lever to reduce the overall energy demand of chemicals production. Conventional strategies to optimize selectivities of thermal reactions comprise the control of the temperature and/or concentration field, whose impact is limited for a given catalytic system. Consequently, major efforts have been put into the development of highly selective catalysts. The conventional way to tailor the catalytic system is frequently empirical and laborious,[2] especially for reactions for which mechanistic understanding is insufficient. Light introduces a new degree of freedom in reaction control, which provides the opportunity to break the parameter correlations in conventional thermo-catalytic reaction control strategies by inducing additional effects. Specifically, high selectivities could be achieved by exploiting such auspicious additional degrees of freedom,[3] which is of utmost importance to minimize raw material and energy demand in the chemical value chain.

Light driven reactions are well known for their high selectivity, but broad large-scale application has not been established yet, mainly due to challenges in scale-up and overall performance of the reactions. Beside photocatalysis, photothermal reactions have gained increasing interest in recent times,[4] but the strong coupling of thermal and electronic effects raises challenges to disentangling these effects. Various studies report a positive impact of light irradiation on the activity and/or selectivity of conventional, thermally initiated heterogeneously catalyzed reactions.[5–7] These studies lump photothermal and photokinetic effects, while Melsheimer et al.[8] clearly attribute higher conversions under irradiation to a pure photothermal effect. Recent theoretical studies have shown that the observed reaction rates in flat-bed reactors are highly sensitive to irradiation and that the differentiation of photothermal and photocatalytic effects requires knowledge of the catalyst

temperature with spatial resolution.[9] Hence, for knowledge-driven tailoring of catalytic systems with optimal performance, a clear differentiation between photothermal, photocatalytic and photoassisted effects is imperative.

Consequently, this study aims at the experimental demonstration of the photoassisted switching of selectivity for heterogeneously catalyzed reactions by irradiation with light. CO_2 hydrogenation on Ru/TiO_2 is chosen as an example, where chain growth determines the selectivity towards various hydrocarbons. To quantify the effect of irradiation on the reaction, a systematic distinction of photothermal, photokinetic and photoassisted effects by sophisticated thermal imaging and kinetic modelling is performed.

Results

The CO_2 hydrogenation towards aliphatic hydrocarbons on Ru/TiO_2 was chosen as a model system for heterogeneously catalyzed gas phase reactions, due to its unique features. First, this reaction system is sufficiently complex with respect to the mechanism and the reaction network.[10] Specifically, the product spectrum is continuously tunable with respect to the hydrocarbon chain length distribution from methanation to Fischer-Tropsch (FT) synthesis via adaption of the operating conditions (e.g., temperature, pressure, H_2/CO_2 ratio).[11] Second, validated kinetic models are available for quantifying the product spectrum characteristics based on unique features of the reaction network.[11,12] For instance, chain growth and termination steps suffice to describe the spectrum based on similarity of the steps irrespective of the specific hydrocarbon chain length.[12] Third, Ru/TiO_2 is reported to exhibit light-induced effects with emphasis on apparent activity,[5,6,8,13,14,15] while it provides high intrinsic activity in CO_2 hydrogenation even at low temperatures.[16,17]

The exothermicity of CO_2 hydrogenation potentially interferes with light-induced effects and thus requires a sound strategy for disentangling the different effects.[9] Specifically, the product spectrum is controlled by the kinetic relation between chain growth and termination, which strongly depends on the reaction temperature and thus on the intrinsic activation energies of the individual reaction steps.[11] Since the exothermicity is potentially amplified by light irradiation,[9] knowledge of the reaction temperature is the key to elucidate the effect of light on CO_2 hydrogenation performance. Hence, CO_2 hydrogenation on Ru/TiO_2 is the ideal model system for systematic experimental studies on light-induced effects in the transition regime between methanation and FT synthesis.

The experimental challenges are addressed with a well-defined planar catalyst and reactor geometry to enable homogeneous irradiation, as well as the measurement of the catalyst surface temperature under reaction conditions and irradiation with light. The reactant consumption rate and product distribution are measured by a gas chromatograph (GC) during continuous operation, following a sophisticated experimental design to distinguish and quantify the effects of irradiation and temperature on the catalytic performance indicators. The well-defined geometry and small thickness of the catalyst layer used justifies the assumption that the measured catalyst surface temperature is representative for the reaction temperature (see supporting information, SI, for Thiele modulus estimation).[9] The differential operation at low conversion further minimizes the effect of undesired temperature gradients. Furthermore, the catalyst surface temperature is used for evaluation and quantification of the catalyst performance indicators with respect to apparent activation energies independent of super-imposed photothermal effects. Diffusive reflectance measurements of the support TiO_2 and the Ru/TiO_2 catalyst shows that about 60 % of the photons incident on the catalyst plate can be absorbed (see Figure S6 in SI). The Ru/TiO_2 catalyst does not show any additional absorption of light in the UV-range in comparison to TiO_2 and thus does not interfere with absorption of UV-light by TiO_2. Radiometric measurements showed a homogenous irradiation of the photocatalyst

with a total incident radiometric power of 0.06 W (see Figure S38 in SI). To elucidate the photoeffect, the catalytic performance indicators are studied for irradiated and dark conditions under continuous reactive gas flow. Therefore, the reaction temperature is increased stepwise from 150 to 200 °C and kept constant for ca. 8 h with alternating irradiated and dark phases of ca. 2 h duration each. This periodic operation provides simultaneous insights into reproducibility as well as catalyst deactivation. The reaction was conducted at 1.5 bar to minimize the formation of higher hydrocarbons.

Figure 1 shows the obtained results for one specific temperature set point. Additional results for the temperature range from 150 to 200 °C are summarized in the SI (Figures S27-S32). The observed responses are well reproducible and no catalyst deactivation is observed during the experimental trials. A clear response of the catalyst surface temperature upon irradiation was measured by infrared (IR) thermal imaging with an IR camera (Figure 1A) with a moderate temperature rise of ca. 3 K compared to the dark phase. Furthermore, the impact of irradiation on the temperature can be distinguished from the small baseline drift observed during the experiments by the IR camera measurements.

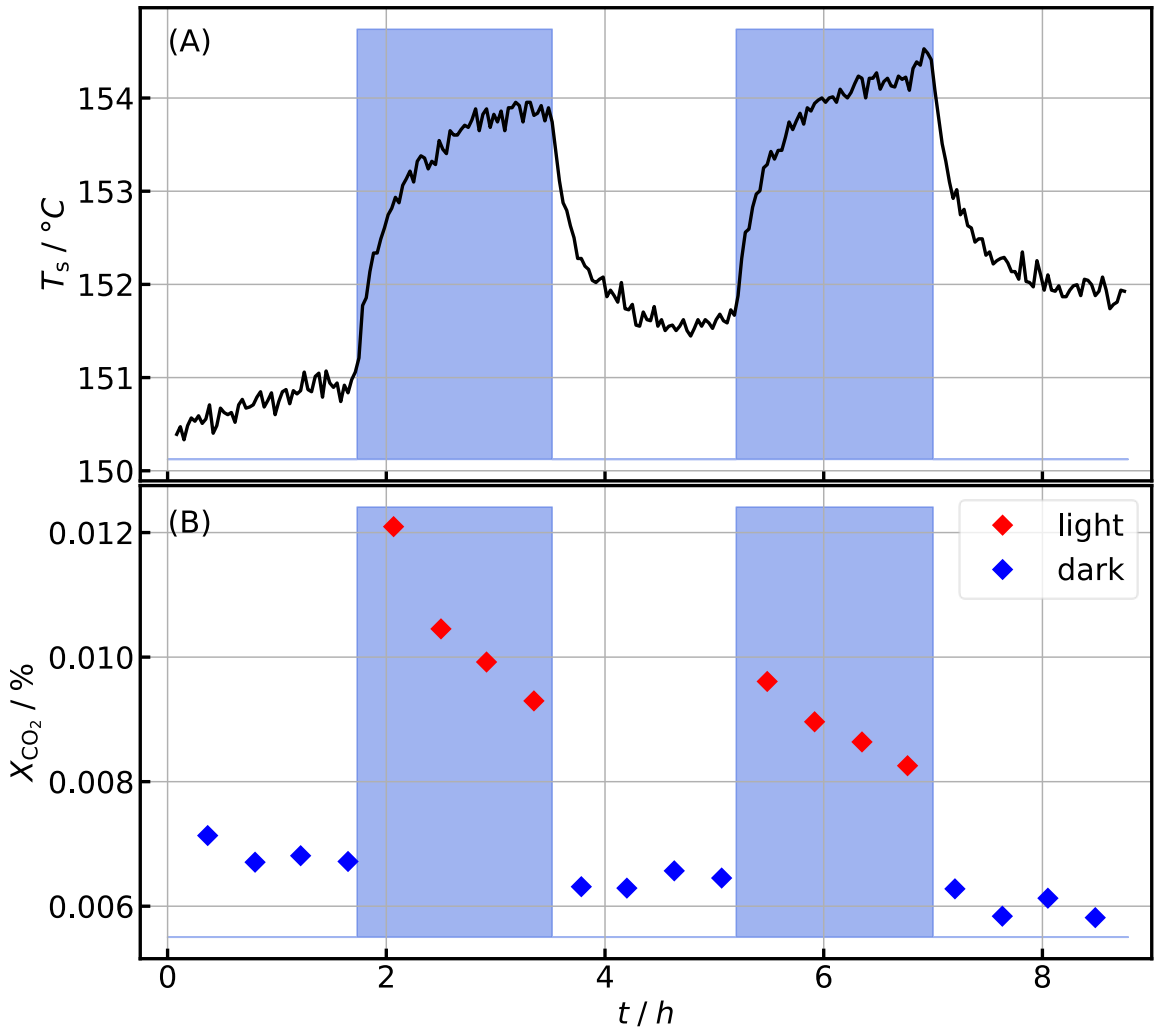

Figure 1: Evolution of (A) surface temperature, T_S, of the catalyst layer measured by IR camera, and (B) CO_2 conversion, X_{CO_2}, over time-on-stream, t; the shading indicates periods of irradiation (conditions: 8.33 mL_{STP} min^{-1} N_2, 33.33 mL_{STP} min^{-1} H_2, 8.33 mL_{STP} min^{-1} CO_2, 150 °C, 1.5 bar, catalyst: 86.8 mg 1 wt.-% Ru/TiO_2, 0.06 W incident radiometric power at 365 nm).

The obtained CO_2 conversion is low but significant (Figure 1B), which justifies assuming differential conditions for the evaluation of the catalyst performance indicators. The Ru particle size of 10 nm determined by H_2 chemisorption is in the optimal range with respect to turn-over-frequency (TOF) expected from CO hydrogenation studies.[18] The TOFs in the present work (e.g., ≈$5 \cdot 10^{-3}$ s^{-1} at 190 °C,

see Table S3 in SI) correspond well to literature-reported results, where values in the range of $10 \cdot 10^{-3}$ s^{-1} to $20 \cdot 10^{-3}$ s^{-1} are reported for CO_2 methanation on Ru/TiO_2 at 190 °C.[19]

The conversion raises under irradiation compared to dark conditions, while the temperature dependencies match well with the Arrhenius equation, independent whether the catalyst is irradiated or not (Figure 2). Quantitative analysis reveals an apparent activation energy of ca. 62 kJ/mol both for the dark and the irradiated case, which is in good agreement with values reported in literature (30,320 Btu/lbmol = 70.52 kJ/mol)[20]. The insignificant effect of irradiation on the activation energy indicates that irradiation causes solely a photothermal effect on the reaction rate and hence on CO_2 conversion, due to temperature increase. Furthermore, the good consistency of the determined activation energy with literature values proves that the measured surface temperature is representative for the reaction temperature and allows to quantify the photothermal effects induced by irradiation. For a set reaction temperature of 150 °C, a CO_2 consumption rate of 6.91 µmol kg^{-1} s^{-1} under irradiation and a rate of 4.61 µmol kg^{-1} s^{-1} under dark conditions is found (based on data in Table S3 in SI based and the catalyst mass used in the experiments).

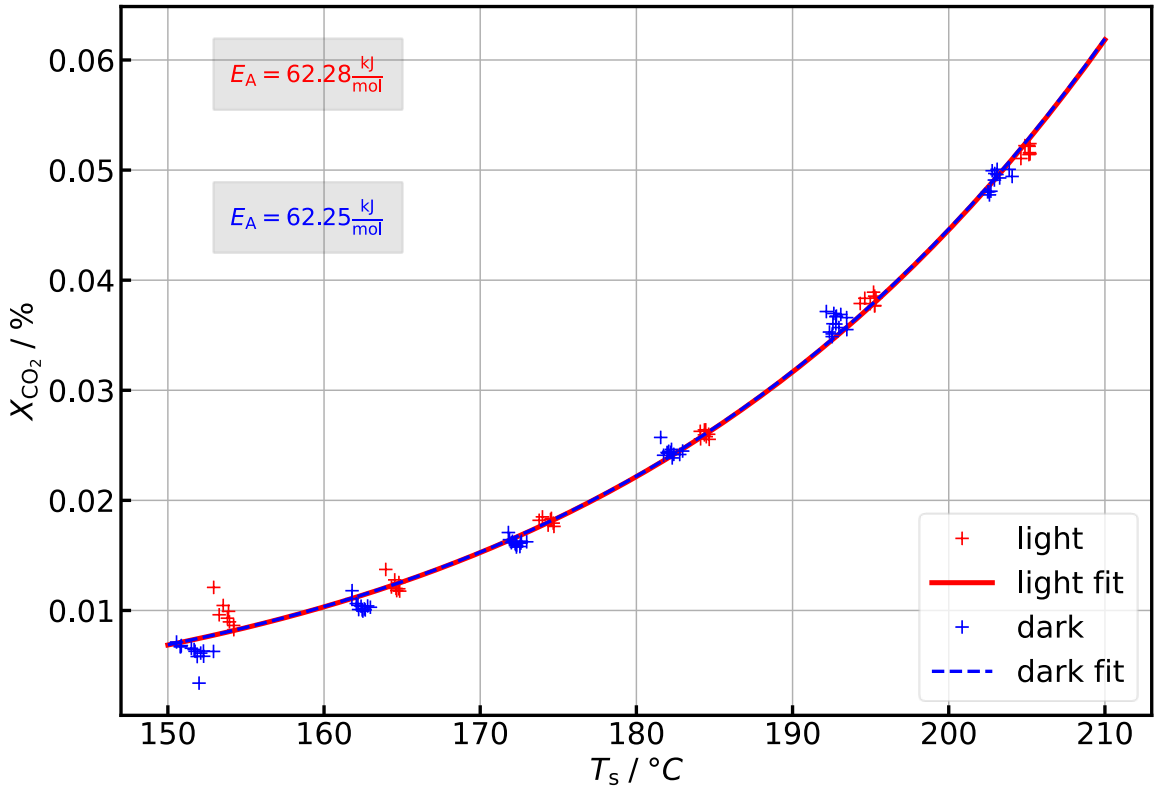

Figure 2: CO_2 conversion, X_{CO_2}, as function of surface temperature, T_S, for the dark case and during irradiation with light; functions are fitted to the experimental data provided in the respective panel (conditions: 8.33 mL_{STP} min^{-1} N_2, 33.33 mL_{STP} min^{-1} H_2, 8.33 mL_{STP} min^{-1} CO_2, 1.5 bar, catalyst: 86.8 mg 1 wt.-% Ru/TiO_2, 0.06 W incident radiometric power at 365 nm).

A sound comparison to literature results is challenging since reaction conditions strongly differ and reported experimental details, especially for the radiation field, e.g., photon flux incident on the catalyst, are frequently insufficient for an objective comparison.[21] One of the rare publications that is comparable to some extent, studied the photocatalytic CO_2 hydrogenation to methane with Ru/TiO_2.[22] A CO_2 consumption rate of 0.33 µmol kg^{-1} s^{-1} under irradiation with a Xe lamp (300 W) at 25 °C and ambient pressure was observed in a batch reactor (apparent quantum yield ≈ 0.07 %). The photocatalytic activity is attributed to a combination of activation of CO_2 on the Ru nanoparticles,[23] localized surface plasmon resonance and subsequent hot electron injection with (photo-)thermal promotion.[24] However, considering that the total CO_2 conversion activity is more than one order of

magnitude higher and that no influence of irradiation on the activation energy is observed in our study, a pure photothermal effect is assumed (Figure 2).

The analysis of the product spectrum with respect to aliphatic hydrocarbons reveals the formation of methane (C_1) together with C_2 and C_{3+} species (Figure 3); C_{3+} are lumped together for evaluation. This selectivity distribution is expected, since ruthenium is known to facilitate chain growth towards the formation of aliphatic hydrocarbons via FT reaction[10,25] and is active for CO or CO_2 hydrogenation.[16] Strikingly, the obtained selectivities show a clear response to irradiation. The methane selectivity drops, while that of the C_{3+} species raises under irradiation. Considering the higher temperature under irradiation, this observation is contradicting the state-of-the-art kinetic understanding on pure thermally activated FT reaction. The methane selectivity usually raises, while the selectivity towards higher hydrocarbons drops with increasing temperature.[26] The influence of irradiation on the C_2 selectivity is small, but observable. Considering that the reaction is conducted at low pressure, the considerable degree of chain growth under irradiation stands out even more.

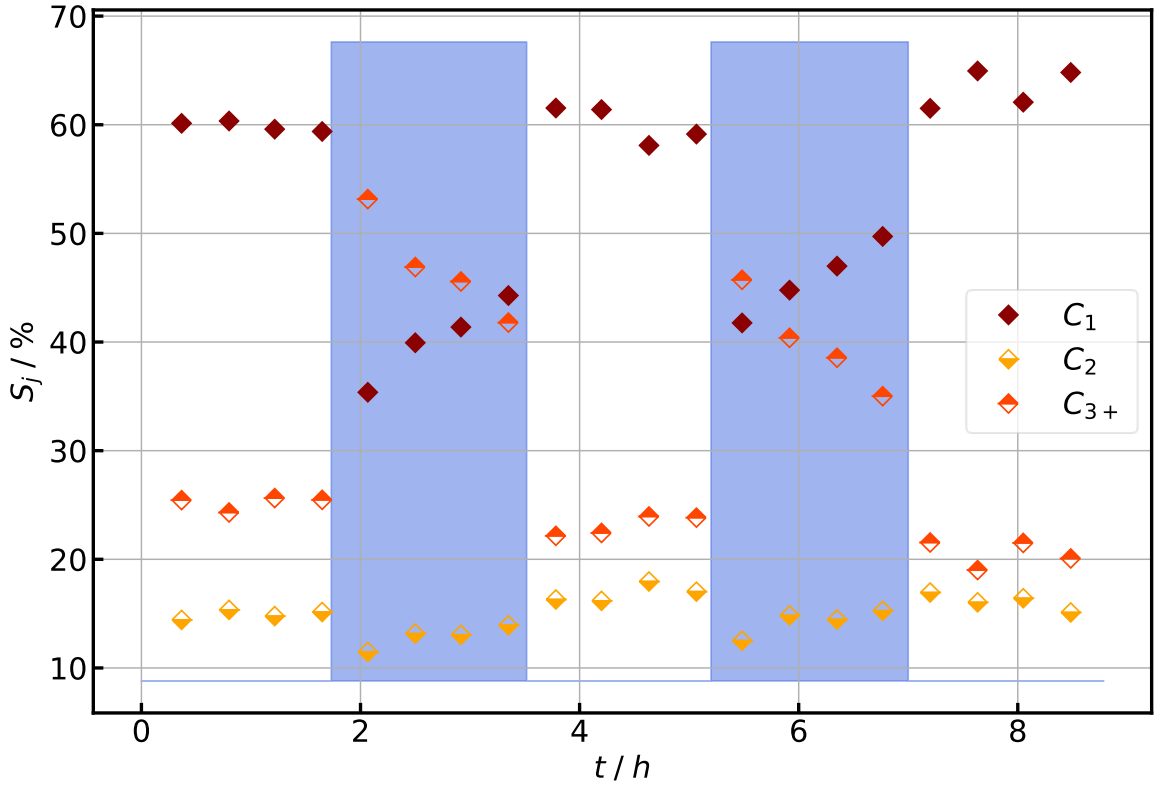

Figure 3: Evolution of the selectivity, S_j, towards methane (C_1), C_2 and C_{3+} hydrocarbons over time-on-stream, t; the shading indicates periods of irradiation (conditions: 8.33 mL_{STP} min^{-1} N_2, 33.33 mL_{STP} min^{-1} H_2, 8.33 mL_{STP} min^{-1} CO_2, 150 °C, 1.5 bar, catalyst: 86.8 mg 1 wt.-% Ru/TiO_2, 0.06 W incident radiometric power at365 nm).

A simplified mechanistical hypothesis of the investigated FT reaction on supported Ru catalysts is derived from literature[10,16] and illustrated in Figure 4. After initial activation of CO_2 on Ru, an adsorbed $CO^\star$ species is formed, which participates in chain growth either directly through the CO insertion or through the carbide mechanism (as precursor for $C_1H_x^\star$). Chain growth proceeds through repeated addition of either $CO^\star$ or $C_1H_x^\star$ to adsorbed $C_nH_m^\star$ species and is terminated by desorption of the hydrocarbon from the catalyst surface. According to Rommens and Saeys,[10] several studies agree that high $CO^\star$ surface coverages facilitate C-C coupling and chain growth. At the same time, high $H^\star$ coverages are expected to favor methane formation by hydrogenation of $C_1H_x^\star$ surface species, which agrees with the proportional relation between methane formation rate and H_2 partial pressure[16].

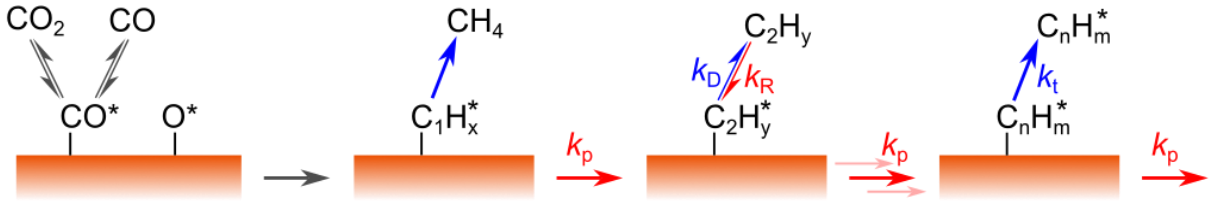

Figure 4: Mechanistic hypothesis for CO_2 activation and hydrocarbon chain growth during CO_2 hydrogenation on ruthenium derived from literature[10,16]; kinetic constants, k_j, for chain propagation (p) and termination (t), as well as for C_2 desorption (D) and re-adsorption (R) are indicated, potential effect of light on reaction step indicated by color code in legend.

The conducted quantitative analysis of the hydrocarbon selectivity is based on kinetic models derived from the mechanism outlined in Figure 4. The models consider the rates of propagation (chain growth), and termination, as well as desorption, and re-adsorption steps according to literature.[11,12] Assuming pseudo zero-order reactions, the chain growth probability, α, can be described with the kinetic constants for propagation, k_p, and termination, k_t, according to eq. (1). The activation energy difference between the propagation and the termination step ($\Delta E_{\mathrm{A},\alpha} = E_{\mathrm{A,p}} - E_{\mathrm{A,t}}$) can be determined by considering the Arrhenius equation for the kinetic constants of both reaction steps (eq. (2)). Accordingly, the C_2 re-adsorption probability, β, is expressed by eq. (3) based on the kinetic constants for C_2 desorption, k_D, and re-adsorption, k_R, with the activation energy difference between the re-adsorption and the desorption step ($\Delta E_{\mathrm{A},\beta} = E_{\mathrm{A,R}} - E_{\mathrm{A,D}}$).

$$\alpha^{-1} = 1 + \frac{k_\mathrm{t}}{k_\mathrm{p}} = 1 + k_{0,\alpha} \exp\left[\frac{E_{\mathrm{A,p}} - E_{\mathrm{A,t}}}{R}\left(\frac{1}{T} - \frac{1}{T_\mathrm{ref}}\right)\right] \tag{1}$$

$$\frac{k_j}{k_{j,\mathrm{ref}}} = k'_{0,j} \exp\left[-\frac{E_{\mathrm{A},j}}{R}\left(\frac{1}{T} - \frac{1}{T_\mathrm{ref}}\right)\right] \tag{2}$$

$$\beta^{-1} = 1 + k_{0,\beta} \exp\left[\frac{E_{\mathrm{A,R}} - E_{\mathrm{A,D}}}{R}\left(\frac{1}{T} - \frac{1}{T_\mathrm{ref}}\right)\right] \tag{3}$$

The chain growth probability, α, declines with raising temperature as expected, while it increases with irradiation (Figure 5A). Hence, chain growth is enhanced at lower temperatures and under irradiation, while termination is enhanced under opposite conditions. The temperature dependency of the chain growth probability is quantified for the dark and the irradiated case by fitting the activation energy difference to the experimental data (for parity plots see Figures S16 in SI). The obtained activation energy difference found for irradiated conditions is smaller compared to the dark case. This means that the activation energy for chain termination raises relatively to that of chain propagation under irradiation. Hence, a reduction in temperature allows to increase chain propagation under irradiations. Furthermore, the C_2 re-adsorption probability, β, raises with temperature and under irradiation (Figure 5B). Under irradiated conditions, the activation energy difference is smaller compared to the dark case, which indicates a lower activation energy for re-adsorption compared to desorption step during irradiation.

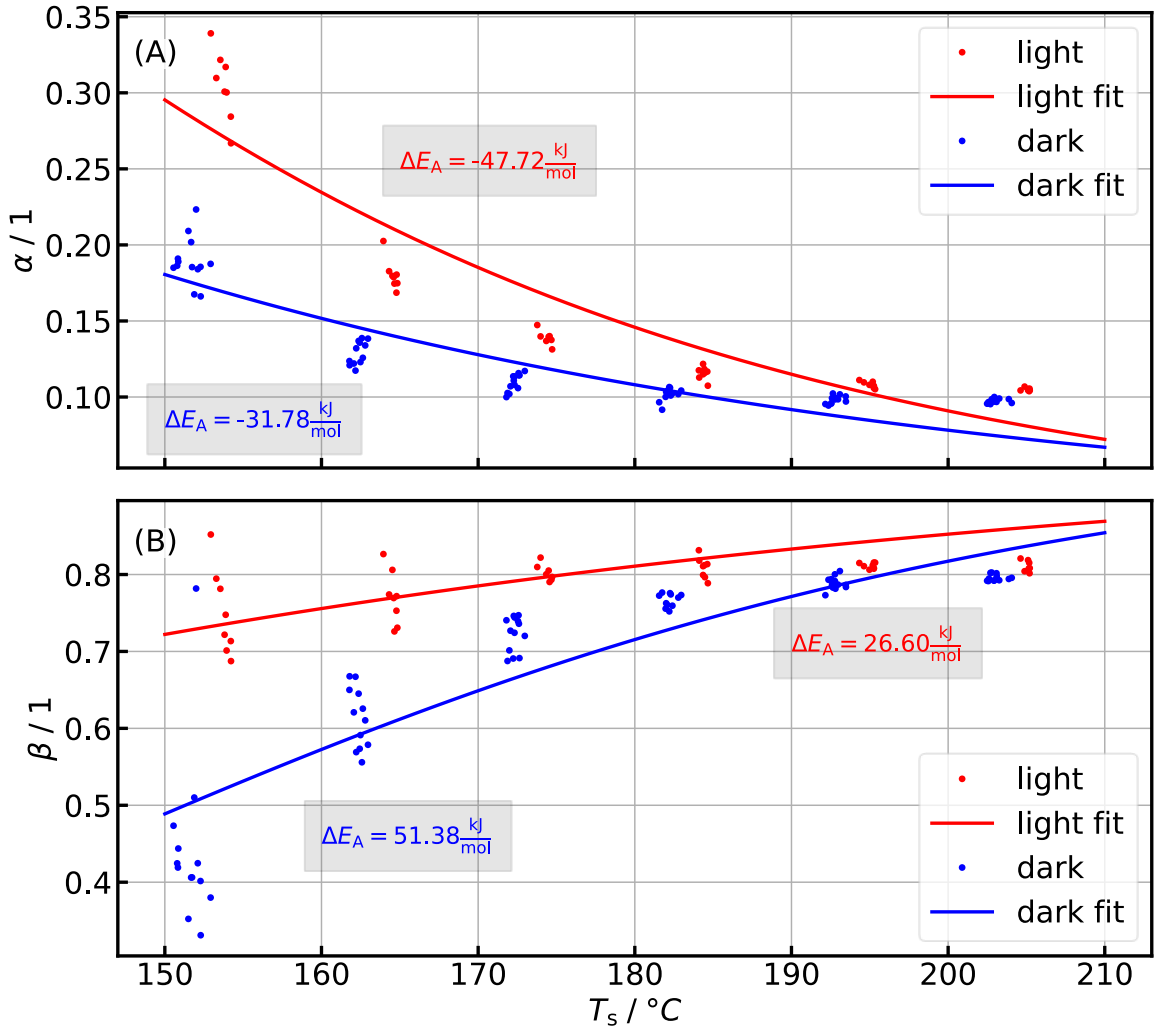

Figure 5: (A) chain growth probability, α, and (B) C_2 re-adsorption probability, β, as function of surface temperature, T_S, for the dark case and during irradiation with light; functions are fitted to the experimental data provided in the respective panel (conditions: 8.33 mL_{STP} min^{-1} N_2, 33.33 mL_{STP} min^{-1} H_2, 8.33 mL_{STP} min^{-1} CO_2, 150 °C, 1.5 bar, catalyst: 86.8 mg 1 wt.-% Ru/TiO_2, 0.06 W incident radiometric power at 365 nm).

Considering the mechanistic hypothesis, it is remarkable that C-C coupling and chain growth is observed already at potentially low $CO^{\star}$ coverage (1.5 bar system pressure) and thus an even lower CO_2 partial pressure of 250 mbar. Furthermore, the high H_2/CO_2 ratio used is expected to favor the formation of CH_4 instead of higher hydrocarbons. An activation of CO_2 by irradiation is not observed, neither directly (higher CO_2 consumption rate) nor indirectly via the primary products CO (no CO detected) or CH_4. Instead, irradiation leads to enhanced chain growth and lower CH_4 selectivity. Therefore, a higher coverage of the intermediates $CO^{\star}$ (and also $C_1H_x^{\star}$) is unlikely the cause for the enhanced chain growth. Instead, it is more likely that the coverage by adsorbed $C_nH_m^{\star}$ species raises under irradiation, which agrees with the detected change in activation energy differences for both chain growth and C_2 re-adsorption. While a higher activity upon irradiation is reported already[13,15] and reasoned by a photothermal effect, the influence of light on chain growth has not been studied yet.

Acceleration of both steps, the chain growth and C_2 re-adsorption, may lead to the increased formation of higher hydrocarbons experimentally observed. This is reflected in the reduced activation barriers numerically found for both chain propagation and C_2 re-adsorption compared to the competing reaction steps under irradiation. The lower activation barrier for C_2 re-adsorption indicates a stronger interaction between adsorbed hydrocarbons and the active surface under irradiated conditions, which leads to longer residence times of the hydrocarbon molecules close to the active centers and therefore

a higher probability for chain growth. Additionally, the simplifying assumption of pseudo-zero-order reactions may cause a correlation between the apparent values determined for activation energy and kinetic constants. For instance, higher coverages with $C_2H_y^\star$ species due to a raising C_2 re-adsorption probability upon irradiation may cause an increased propagation rate, which leads to higher values for the respective kinetic constant assuming a zero-order reaction. This effect is superimposed by the raise in kinetic constant with temperature, as expressed by the Arrhenius equation, which may cause the drop in apparent activation energy. Furthermore, it is known that irradiation with light affects the sorption properties of solid surfaces. For instance, irradiation leads to the formation of surface hydroxyl groups on TiO_2 in the presence of H_2O.[27] Therefore, it is plausible to assume that specific adsorption steps during CO_2 hydrogenation and chain growth (e.g., C_2 re-adsorption) are favored by irradiation. Hence, the experimental observations agree with mechanistic considerations and the obtained apparent kinetic parameters. Consequently, it is assumed that irradiation changes the coverages of surface species during the reaction, which finally promotes chain growth. Simultaneously, the activation of CO_2 and H_2 is not affected by the presence of light and appears to be purely thermally driven.

The scientific discussion in literature currently considers the use of light either to initiate reactions by electronic excitation of a molecule/solid or to provide thermal energy through radiation. All applications that use the first principle might be categorized as photokinetic use of photons, meaning that the rate of reaction can be correlated with the incident photon flux and the quantum yield. The second principle simply utilizes conversion of photons into thermal energy and thus corresponds to a photothermal use of photons. Hence, the significant change in C_2 re-adsorption and chain growth probability observed in this work is neither a photokinetic nor a photothermal use of photons. Consequently, another principle of a photoassisted use of photons is proposed here, which requires further elaboration.

Conclusion

The obtained results clearly demonstrate the capabilities of irradiation with light to switch selectivity for the example of CO_2 hydrogenation on Ru/TiO_2 catalysts. Based on the developed sophisticated experimental and kinetic analysis, a photoassisted mechanism has been revealed that facilitates the chain growth probability and affects the sorption behavior of hydrocarbons, while excluding conventional photokinetic and photothermal effects. The novel concept of photoassisted switching of selectivites is solely related to the interaction of reactants with the solid surface and thus a general applicability is expected, providing additional degrees of freedom for control of chemical reactions.

The observations pave the way to realize process intensification by using light for reaction control by switching selectivity. Therefore, the specific mechanisms for the role of photons in the catalytic cycle need to be elucidated and quantified, to tailor the product distribution of heterogeneously catalyzed reactions. The present work points at selective modification of the interaction between the reactive molecules and the solid surface as major lever, which can be exploited by the non-stoichiometric presence of photons already.

Methods

The experimental methods with respect to catalyst preparation and characterization, reactor setup and analytics, reaction experiments, radiometry and data evaluation are described in detail in the supporting information (SI). Furthermore, additional results are provided in the SI, as well.

The 1 wt.-% Ru/TiO_2 catalyst is synthesized via impregnating TiO_2 (VP Aeroperl P25/20, Evonik) with an ethanolic solution of $RuCl_3 \cdot H_2O$ (97 %, Thermo Scientific). The obtained suspension is applied to a

planar aluminum carrier sheet (1 x 25 x 50 mm^3) exhibiting etched holes with a diameter of 1.2 mm and a depth of 115 µm via the doctor blade method followed by drying at 85 °C and calcination at 200 °C. This procedure provides mechanical stable catalyst layers on the support with defined thickness and external surface area exposed to light irradiation.

The catalyst was characterized by N_2 physisorption, temperature-programmed reduction (TPR), and volumetric H_2 chemisorption performed with a 3-Flex gas analyzer (Micromeritics Instrument Corporation). Physisorption experiments were performed at boiling temperature of N_2 using 50 mg of the porous solid material after degassing at up to 240 °C. Both, the ad- and desorption isotherms were recorded in a relative pressure range of ca. 10^{-2} to 1. The Brunauer-Emmet-Teller (BET) surface area amounts to ca. 53.5 m^2/g and the total pore volume to 0.406 cm^3/g for both, the Ru/TiO_2 catalyst and the TiO_2 support material. For TPR experiments ca. 120 to 220 mg of solid material were dried at 120 °C under Ar prior to heating the samples from 35 °C to 900 °C with a heating rate of 10 K/min under a continuous flow of 10 vol.% H_2 in Ar. The results confirm that the Ru precursor is reduced to metallic Ru at 200 °C. The determination of the metallic Ru surface area was performed using volumetric H_2 chemisorption experiments. Therefore, the materials were reduced at 200 °C under H_2 for 16 h and degassed at 300 °C for 3 h before the H_2 adsorption isotherm was recorded at 50 °C. The layer of spent catalysts was characterized by optical and confocal laser scanning microscopy (VK-X110, Keyence Deutschland GmbH) with respect to the surface and the average catalyst layer thickness. The latter amounts to ca. 165 µm.

The catalyst layer with 86.8 mg of catalyst is positioned in a slit-shaped, self-made reactor, which is put inside of the reactor oven and attached to the gas manifold and outlet. The top half of the reactor is equipped with a quartz window of 4 mm thickness and the oven lid with two 2 mm quartz windows that enables an effective irradiation with UV-light. For irradiation with UV-light, 18 365nm LEDs, operated at a total electrical power of 30.6 W are arranged in a 3 by 6 array atop of the reactor oven window perpendicular to the external surface of the catalyst layer. The radiation field was characterized by 3D-radiometric measurements with a radiometry setup developed in-house.[28] The calibration is based on measurements of individual LEDs with an integrating sphere. With measurements of the bare light source and all optical components installed at different distances, the radiation field on the catalyst surface could be determined by geometrical projection. A radiometric power incident on the catalyst surface of 0.06 W was determined. For measurement of the catalyst surface temperature, an IR-camera (ImageIR® 8300 hs, InfraTec GmbH) with optical access through a slanted sapphire window in the oven (2 mm thick) and the reactor window is installed with an angle of ca. 43° with respect to irradiation. Calibration of the IR camera is performed using a representative catalyst arrangement and a thermocouple placed directly at the external surface of the catalyst layer.

The reactor is operated under continuous gas flow supplied by mass flow controllers (EL-Flow, Bronkhorst High-Tech B.V.). The operation pressure of up to 1.5 bar is adjusted by a pressure controller (EL-Press, Bronkhorst High-Tech B.V.). The outlet gas composition with respect to the molar fractions of CO_2, CO, CH_4 and C_2 to C_7 species is analyzed by means of an online gas chromatograph (Trace 1310, Thermo Fischer Scientific Inc.) equipped with a thermal conductivity (TCD) and a flame ionization detector (FID) and appropriate columns for separation.

Prior to reaction experiments, the catalyst is reduced in the reactor at 200 °C for 16 h under pure H_2 flow at 1 bar. The reaction experiments are performed under 1.5 bar and a continuous flow of 8.33 mL_{STP}/min of N_2 (5.0 purity, MTI), 33.33 mL_{STP}/min of H_2 (5.0 purity, MTI) and 8.33 mL_{STP}/min of CO_2 (4.8 purity, MTI). Six temperature levels were investigated in the experimental reaction campaign, ranging from 150 to 200 °C with an interval of 10 K. At every temperature level two light and three dark phases are realized with a duration of ca. 2 h each, in order to realize 4 GC sampling events. Therefore,

light was initially switched off, followed by repeating the on-off sequence twice, which leads to an overall duration of approx. 8 to 10 h per temperature level. For safety reasons, the reactor feed was switched to an inert stream of 20 % H_2 in N_2 (2 mL_{STP}/min of H_2 and 8 mL_{STP}/min of N_2) overnight. Hence, the time-on-stream is only cumulated for actual syngas fed to the reactor. Potential deactivation was accounted for by repeated measurements at 150 °C.

The CO_2 conversion, X_{CO_2}, is calculated with eq. (4) based on the molar fractions of each hydrocarbon species, x_i, obtained from GC data of the FID channel. This approach is chosen due to the low conversion, which results in very small differences in the CO_2 concentration between inlet and outlet. Due to the low conversion, the total inlet and outlet molar flow rates are nearly identical and the error introduced by this approximation is sufficiently small. In eq. (4) the inlet and outlet molar flow rates of CO_2, $\dot{n}_{CO_2,in}$ and $\dot{n}_{CO_2,out}$, the inlet molar fraction of CO_2, $x_{CO_2,in}$, and the carbon number, $n_{i,C}$, is used. The activation energy, E_A, of the main reaction is estimated numerically from the CO_2 conversion using the Arrhenius equation. This is justified by the low conversion, which allows to assume pseudo-zero order reaction kinetics.

$$X_{CO_2} = \frac{\dot{n}_{CO_2,in} - \dot{n}_{CO_2,out}}{\dot{n}_{CO_2,in}} \approx \frac{1}{x_{CO_2,in}} \sum_{i=CH_4}^{C_7H_{16}} \frac{x_i}{n_{i,C}} \tag{4}$$

The TOF was calculated from the inlet CO_2 molar flow rate, $\dot{n}_{CO_2,in}$, the CO_2 conversion, X_{CO_2}, the specific molar amount of adsorbed H_2, n_{H_2} (5 µmol/g, measured by volumetric chemisorption), and the catalyst mass, m_{cat} (86.8 mg, set value), according to eq. (5). The number of active sites assumed for the TOF estimation is expressed by $n_{H_2} \cdot m_{cat}$. The inlet CO_2 molar flow rate is calculated from the inlet CO_2 volumetric flow rate (8.33 mL_{STP} min^{-1}, set value) with standard temperature and pressure and the ideal gas constant.

$$\mathrm{TOF} = \frac{\dot{n}_{CO_2,in}\, X_{CO_2}}{n_{H_2}\, m_{cat}} \tag{5}$$

The selectivity towards CH_4 (S_{C_1}), C_2 (S_{C_2}), and C_{3+} ($S_{C_{3+}}$) species is calculated by eqs. (6) and (7) from measured molar fractions of each hydrocarbon. In these groups, all hydrocarbons with the same carbon number, e.g., paraffins, olefins and isomers, were lumped together.

$$S_{C_n} = \frac{1}{n} \sum_j x_{j,n} \left(\sum_{i=CH_4}^{C_7H_{16}} \frac{x_i}{n_{i,C}} \right)^{-1} \quad \text{for } n \in [1,2] \tag{6}$$

$$S_{C_{3+}} = 1 - \left(S_{C_1} + S_{C_2} \right) \tag{7}$$

The hydrocarbon distribution is assumed to follow the modified Anderson-Schulz-Flory (ASF) distribution proposed by Förtsch et al.,[12] with the chain growth probability, α, the re-adsorption probability, β, and the enhanced termination probability for methane, γ. The ASF parameters α and β are obtained by numerical estimation based on the measured selectivities and the hydrocarbon distribution model. The parameter γ is assumed zero. The activation energies of the ASF parameters are determined by numerical estimation with eqs. (1) to (3). Numerical parameter estimation is performed using Python and the *scipy.optimize.least_squares* method.

Acknowledgements

The authors thank the Vector Stiftung for financial support within the Light-2-Gas project (P2018-0118) as well as Carsten Streb and Sven Rau for scientific discussion. Furthermore, thanks go to the Institute of Chemical and Electrochemical Process Engineering, TU Clausthal, Germany and CUTEC Forschungszentrum, TU Clausthal, Germany for support with material characterization. DZ thanks the Deutsche Forschungsgemeinschaft for support by the collaborative research center TRR234 "CataLight" (364549901), project C6 as well as Alina Koba and Daniel Kowalczyk for help on the radiometric measurements. RG thanks Deutsche Forschungsgemeinschaft for funding the experimental setup within the Major Research Instrumentation Programme (INST 40/516-1 FUGG). Furthermore, we thank our student Lorraine Arzner for their valuable contribution to the scientific results.

References

[1] A. Olivier, A. Desgagnés, E. Mercier, M. C. Iliuta, *Ind. Eng. Chem. Res.* **2023**, *62*, 5714.

[2] a) P. Munnik, P. E. de Jongh, K. P. de Jong, *Chem. Rev.* **2015**, *115*, 6687; b) H. Jahangiri, J. Bennett, P. Mahjoubi, K. Wilson, S. Gu, *Catal. Sci. Technol.* **2014**, *4*, 2210.

[3] a) F. Guba, F. Gaulhofer, D. Ziegenbalg, *J. Flow. Chem.* **2021**, *11*, 495; b) M. Sender, F. L. Huber, M. C. G. Moersch, D. Kowalczyk, J. Hniopek, S. Klingler, M. Schmitt, S. Kaufhold, K. Siewerth, J. Popp et al., *ChemSusChem* **2022**, *15*, e202200708.

[4] a) F. Fresno, A. Iglesias-Juez, J. M. Coronado, *Top. Curr. Chem.* **2023**, *381*, 21; b) L. Liao, G. Xie, X. Xie, N. Zhang, *J. Phys. Chem. C* **2023**, *127*, 2766; c) J. Ma, J. Yu, G. Chen, Y. Bai, S. Liu, Y. Hu, M. Al-Mamun, Y. Wang, W. Gong, D. Liu et al., *Adv. Mater.* **2023**, e2302537; d) I. S. Khan, D. Mateo, G. Shterk, T. Shoinkhorova, D. Poloneeva, L. Garzón-Tovar, J. Gascon, *Angew. Chem. Int. Ed.* **2021**, *60*, 26476; e) R. Song, Z. Li, J. Guo, P. N. Duchesne, C. Qiu, C. Mao, J. Jia, S. Tang, Y.-F. Xu, W. Zhou et al., *Angew. Chem. Int. Ed.* **2023**, *62*, e202304470; f) Y. Miao, Y. Zhao, G. I. N. Waterhouse, R. Shi, L.-Z. Wu, T. Zhang, *Nat. Commun.* **2023**, *14*, 4242.

[5] K. R. Thampi, J. Kiwi, M. Grätzel, *Nature* **1987**, *327*, 506.

[6] Q. Li, H. Wang, M. Zhang, G. Li, J. Chen, H. Jia, *Angew. Chem. Int. Ed.* **2023**, *62*, e202300129.

[7] G. E. O'Connell, T. H. Tan, J. A. Yuwono, Y. Wang, A. Kheradmand, Y. Jiang, P. V. Kumar, R. Amal, J. Scott, E. C. Lovell, *Appl. Catal., B* **2024**, *343*, 123507.

[8] J. Melsheimer, W. Guo, D. Ziegler, M. Wesemann, R. Schlögl, *Catal. Lett.* **1991**, *11*, 157.

[9] H. Becker, D. Ziegenbalg, R. Güttel, *Catal. Sci. Technol.* **2023**, *13*, 645.

[10] K. T. Rommens, M. Saeys, *Chem. Rev.* **2023**, *123*, 5798.

[11] D. Vervloet, F. Kapteijn, J. Nijenhuis, J. R. van Ommen, *Catal. Sci. Technol.* **2012**, *2*, 1221.

[12] D. Förtsch, K. Pabst, E. Groß-Hardt, *Chem. Eng. Sci.* **2015**, *138*, 333.

[13] Y. Li, Z. Liu, Z. Rao, F. Yu, W. Bao, Y. Tang, H. Zhao, J. Zhang, Z. Wang, J. Li et al., *Appl. Catal., B* **2022**, *319*, 121903.

[14] a) X.-N. Guo, Z.-F. Jiao, G.-Q. Jin, X.-Y. Guo, *ACS Catal.* **2015**, *5*, 3836; b) J. Zhao, J. Liu, Z. Li, K. Wang, R. Shi, P. Wang, Q. Wang, G. I. N. Waterhouse, X. Wen, T. Zhang, *Nat. Commun.* **2023**, *14*, 1909; c) A. V. Puga, *Top. Catal.* **2016**, *59*, 1268.

[15] L. Lin, K. Wang, K. Yang, X. Chen, X. Fu, W. Dai, *Appl. Catal., B* **2017**, *204*, 440.

[16] H. Mansour, E. Iglesia, *J. Am. Chem. Soc.* **2021**, *143*, 11582.

[17] a) J. Ilsemann, M. M. Murshed, T. M. Gesing, J. Kopyscinski, M. Bäumer, *Catal. Sci. Technol.* **2021**, *11*, 4098; b) J. Zhou, Z. Gao, G. Xiang, T. Zhai, Z. Liu, W. Zhao, X. Liang, L. Wang, *Nat. Commun.* **2022**, *13*, 327; c) S. Cisneros, S. Chen, C. Fauth, A. M. Abdel-Mageed, S. Pollastri, J. Bansmann, L. Olivi, G. Aquilanti, H. Atia, J. Rabeah et al., *Appl. Catal., B* **2022**, *317*, 121748.

[18] a) J. M. G. Carballo, J. Yang, A. Holmen, S. García-Rodríguez, S. Rojas, M. Ojeda, J. L. G. Fierro, *J. Catal.* **2011**, *284*, 102; b) J. L. Eslava, X. Sun, J. Gascon, F. Kapteijn, I. Rodríguez-Ramos, *Catal. Sci. Technol.* **2017**, *7*, 1235.
[19] A. M. Abdel-Mageed, K. Wiese, M. Parlinska-Wojtan, J. Rabeah, A. Brückner, R. J. Behm, *Appl. Catal., B* **2020**, *270*, 118846.
[20] P. J. Lunde, F. L. Kester, *Ind. Eng. Chem. Proc. Des. Dev.* **1974**, *13*, 27.
[21] D. Ziegenbalg, A. Pannwitz, S. Rau, B. Dietzek-Ivanšić, C. Streb, *Angew. Chem. Int. Ed.* **2022**, *61*, e202114106.
[22] E. Morais, C. O'Modhrain, K. R. Thampi, J. A. Sullivan, *Int. J. Photoenergy* **2019**, *2019*, 1.
[23] C. Kim, S. Hyeon, J. Lee, W. D. Kim, D. C. Lee, J. Kim, H. Lee, *Nat. Commun.* **2018**, *9*, 3027.
[24] D. Mateo, J. L. Cerrillo, S. Durini, J. Gascon, *Chem. Soc. Rev.* **2021**, *50*, 2173.
[25] a) V. V. Ordomsky, A. Y. Khodakov, B. Legras, C. Lancelot, *Catal. Sci. Technol.* **2014**, *4*, 2896; b) J. M. González Carballo, E. Finocchio, S. García, S. Rojas, M. Ojeda, G. Busca, J. L. G. Fierro, *Catal. Sci. Technol.* **2011**, *1*, 1013; c) A. V. Puga, *Catal. Sci. Technol.* **2018**, *8*, 5681.
[26] X.-Y. Quek, R. Pestman, R. A. van Santen, E. J. M. Hensen, *Catal. Sci. Technol.* **2014**, *4*, 3510.
[27] M. Qu, G. Huang, X. Liu, X. Nie, C. Qi, H. Wang, J. Hu, H. Fang, Y. Gao, W.-T. Liu et al., *Chem. Sci.* **2022**, *13*, 10546.
[28] a) M. Sender, B. Wriedt, D. Ziegenbalg, *React. Chem. Eng.* **2021**, *6*, 1601; b) M. Sender, D. Ziegenbalg, *React. Chem. Eng.* **2021**, *6*, 1614.